We are IntechOpen, the world's leading publisher of Open Access books Built by scientists, for scientists

4,800
Open access books available

122,000
International authors and editors

135M
Downloads

Our authors are among the

154
Countries delivered to

TOP 1%
most cited scientists

12.2%
Contributors from top 500 universities

CLARIVATE ANALYTICS BOOK CITATION INDEX INDEXED

WEB OF SCIENCE™

Selection of our books indexed in the Book Citation Index in Web of Science™ Core Collection (BKCI)

Interested in publishing with us?
Contact book.department@intechopen.com

Numbers displayed above are based on latest data collected.
For more information visit www.intechopen.com

10

Ruthenium(II)-Pyridylamine Complexes Having Functional Groups via Amide Linkages

Soushi Miyazaki[1] and Takahiko Kojima[2]
[1]*Research Center for Materials Science, Nagoya University*
[2]*Department of Chemistry, University of Tsukuba*
Japan

1. Introduction

Functionalization of metal complexes by introduction of functional groups has been recognized to be important toward the development of further functionality of metal complexes, including ion sensing, molecular recognition, and selective catalysis.
Convergence of functional groups into certain direction and appropriate spatial arrangement can be achieved by coordination of metal ions to ligands with those groups to perform novel functions that cannot be achieved by organic ligand molecules for themselves. This strategy allows us to access multifunctional molecules more easily than that with well-designed organic molecules in terms of synthetic availability.
Ruthenium complexes bearing chelating pyridylamine ligands are robust enough to hold those ligands in the coordination spheres for the convergence of functional groups attached to the ligands and to maintain their appropriate spatial geometry. We have used tris(2-pyridylmethyl)amine (TPA) and its derivatives which coordinate to the ruthenium ion as tetradentate ligands. Introduction of functional groups to the 6-position of pyridine rings of TPA can provide additional functionality for ruthenium-TPA complexes (Figure 1). The concept, i.e., the introduction of amide groups at the 6-positions of pyridine rings in TPA, has been originally introduced by Masuda and coworkers to construct a hydrophobic and sterically protected environment in copper complexes by using pivaloylamide groups (Harata *et al*., 1994, 1995, 1998; Wada *et al*., 1998). They have succeeded in a number of important metal complexes in bioinorganic chemistry. Inspired by their works, we have developed our concept to functionalize ruthenium-TPA complexes by introducing various functional groups via amide linkages. In our case, the ruthenium complexes bearing tri-substituted TPA is not suitable for functionalization due to its large steric crowding. Therefore we have applied bisamide and monoamide-TPA as ligands. In this chapter, we will present an overview of a chemistry of ruthenium complexes bearing bisamide-TPA and monoamide-TPA as ligands and their characteristics.

2. Convergence of hydrophobic functional groups in the coordination sphere of ruthenium complexes

According to the strategy mentioned above, we introduced hydrophobic groups to TPA toward molecular recognition based on van der Waals interactions in the coordination

sphere of Ru(II) complexes. The TPA derivatives synthesized were those having 1-naphtyl, 2-naphtyl, and isobutyl groups via amide linkages (*N*,*N*-bis(6-(1-naphthoylamide)-2-pyridylmethyl)-*N*-(2-pyridylmethyl)amine = (1-Naph)$_2$-TPA, *N*,*N*-bis(6-(2-naphthoyl-amide)-2-pyridylmethyl)-*N*-(2-pyridylmethyl)amine = (2-Naph)$_2$-TPA, *N*,*N*-bis(6-(iso-butyrylamide)-2-pyridylmethyl)-*N*-(2-pyridyl-methyl)amine = (Isob)$_2$-TPA, *N*-(6-(1-naphthoylamide)-2-pyridylmethyl)-*N*,*N*-bis(2-pyridylmethyl)amine = 1-Naph-TPA) and their Ru(II) complexes ([RuCl((1-Naph)$_2$-TPA)]PF_6 (**1**), [RuCl((2-naph)$_2$TPA)]PF_6 (**2**), [RuCl((Isob)$_2$-TPA)]PF_6, (**3**), [RuCl((1-Naph)-TPA)(DMSO)]PF_6 (**4**)) were also prepared, respectively (Figure 1) (Kojima *et al.*, 2000, 2004a, 2005).

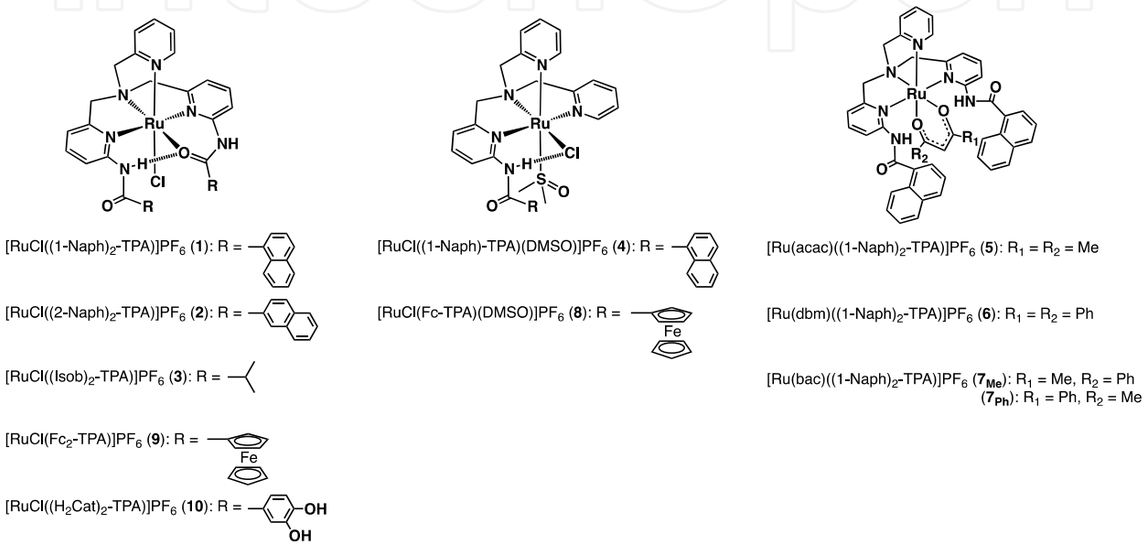

Fig. 1. Structures of Ru-bisamide-TPA and Ru-monoamide-TPA complexes

2.1 Crystal structures of ruthenium(II) complexes bearing TPA with 1-naphthyl, 2-naphthyl, and isopropyl groups via amide linkages

The crystal structures of **1-3** are shown in Figure 2. Those Ru(II)-bisamide-TPA complexes have basically the same coordination environment around the Ru(II) centers. The bisamide-TPA ligands in those complexes coordinate to the Ru(II) ions as pentadentate ligands by the chelation involving three pyridine nitrogen atoms, one tertiary amino nitrogen, and one amide oxygen. Besides those, one chloride ion binds to the Ru(II) center at the *trans* position to the unsubstituted pyridine ring, providing distorted octahedral environments of the Ru(II) complexes. The amide oxygen coordinates to the *trans* site to the tertiary amino nitrogen to afford an asymmetric geometry of the complex. The substituted pyridine rings are located at *trans* positions to each other, and the N-H hydrogen atoms of the uncoordinated amide moiety forms intramolecular hydrogen bonding with the coordinated oxygen atom. The hydrophobic groups were converged and fixed into one direction due to the intramolecular hydrogen bond between two amide arms.

In the structure of **1** (Figure 2a), the bond lengths between the Ru(II) center and the nitrogen atoms of the substituted pyridines are different from the Ru(II) complexes with unsubstituted TPA, reflecting the asymmetric coordination environment due to the coordination of amide oxygen (1.992(5) Å for Ru1-N3 and 2.125(5) Å for Ru1-N4). The

dihedral angles between the amide moieties and the amide-linked pyridine rings are 13.4° for the coordinated amide group and 4.3° for the uncoordinated group, respectively. Compared to those dihedral angles, the naphthalene rings show larger dihedral angels with respect to the amide moieties (39.3° for the coordinated amide and 45.6° for the uncoordinated amide). The coordinated amide oxygen and the uncoordinated amide N-H hydrogen forms the intramolecular hydrogen bond with the distance of 3.036(6) Å for O1···N6 to converge the two naphthyl groups. The two naphthalene rings are close enough to form intramolecular π-π interactions as represented by the shortest contact of 3.36(1) Å for C29-C34 and other interatomic distance are listed in Table 1, and are almost parallel to each other with the dihedral angle of 5.9°, indicating the formation of a face-to-face π-π interaction (Figure 3a) (Hunter & Sanders, 1990; Janiak, 2000). Complex **2** bearing two 2-naphthyl groups exhibits almost the same structural features as those of **1** (Figure 2b). Dihedral angles between the amide-linked pyridine ring and the amide plane were calculated to be 10.4 and 20.7° for the coordinated and the uncoordinated ones, respectively. The distortion between the amide planes and the naphthalene rings (20.6° for the coordinated amide and 20.0° for the uncoordinated amide) are smaller than those observed for **1**, probably due to the lack of steric hindrance derived from the peri hydrogen atoms in **1**. The distance of the hydrogen bond between the coordinated amide oxygen and the

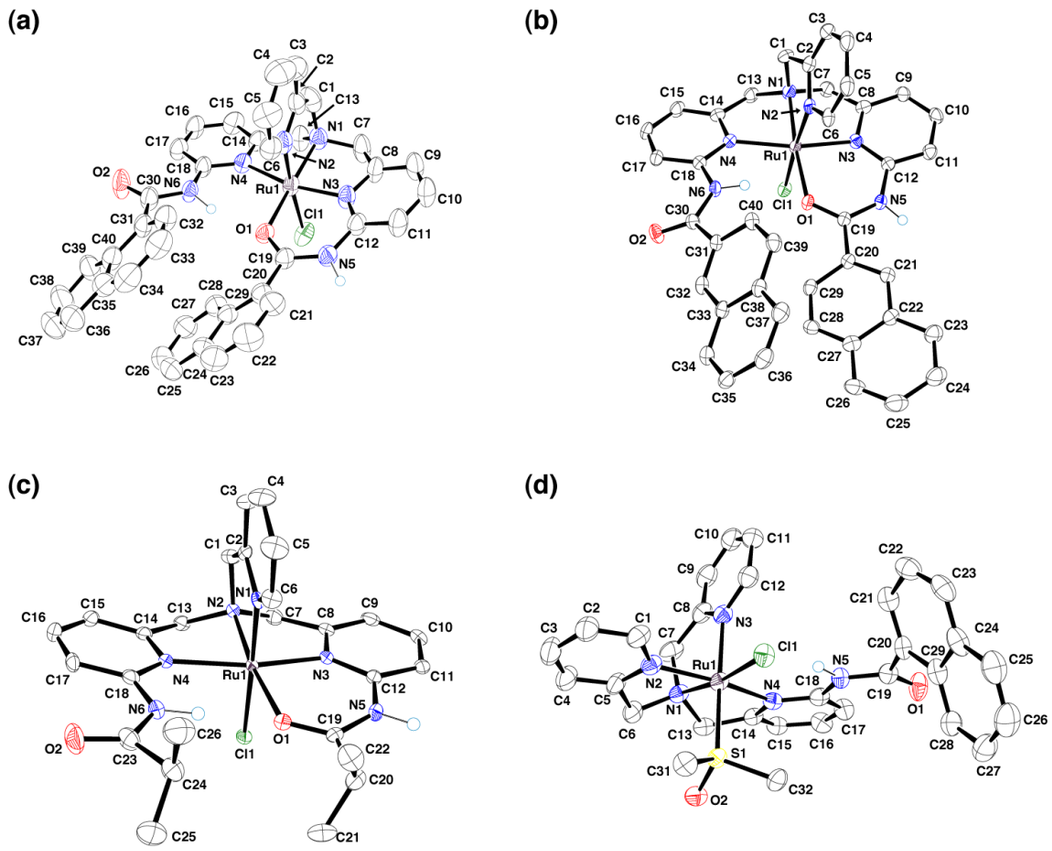

Fig. 2. Crystal structures of the cationic moieties of (a) **1**, (b) **2**, (c) **3**, and (d) **4** with 50% probability thermal ellipsoids. Hydrogen atoms except the amide N-H ones are omitted for clarity.

	1		2
C20···C33	3.68(1)	C26···C32	3.699(4)
C24···C34	3.65(1)	C26···C39	3.528(4)
C24···C35	3.50(1)	C26···C40	3.496(4)
C24···C40	3.43(1)	C27···C31	3.466(4)
C25···C35	3.63(1)	C27···C37	3.596(4)
C25···C40	3.59(1)	C27···C38	3.398(4)
C26···C38	3.69(1)		
C26···C39	3.57(1)		
C27···C31	3.61(1)		
C28···C32	3.64(1)		
C28···C33	3.563(9)		
C29···C33	3.65(1)		
C29···C34	3.36(1)		

Table 1. Interatomic Distances (Å) for Intramolecular π–π Interactions in **1** and **2**.

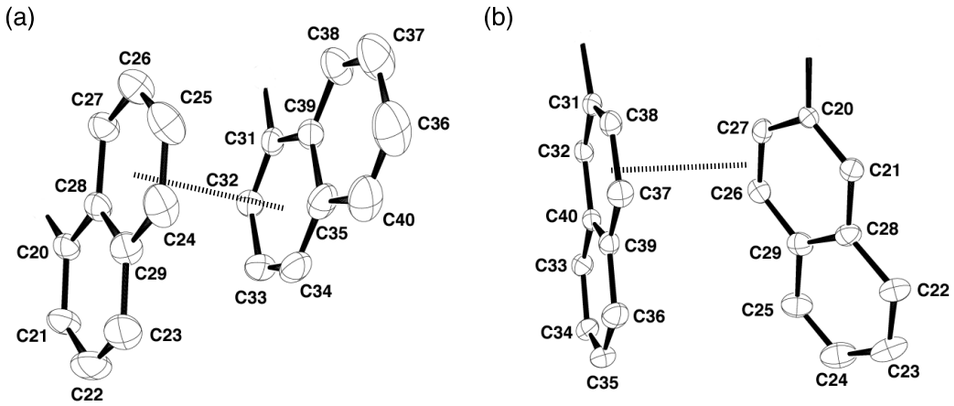

Fig. 3. Intramolecular π-π interactions between two naphthalene rings of (a) **1** and (b) **2**.

uncoordinated amide N-H moiety is 2.977(3) Å (O1···N6). Two naphthalene rings were converged with the shortest contact of 3.398(4) Å for C27-C38. However, two naphthalene rings of **2** show a larger dihedral angle of 27.1° than that (5.9°) of **1**, indicating a sort of edge-to-face π-π interaction (Figure 3b and Table 1). In this complex, the 2-naphthyl groups exhibit fluxional behavior and the thermodynamic parameters of the π-π interaction has been estimated to be $\Delta H°$ = –2.3 kJ mol^{-1}; thus, $\Delta G°$ = –0.9 kJ mol^{-1} and $\Delta S°$ = –7.7 J mol^{-1} K^{-1} at 233 K in CD_3CN.

Concerning the crystal structure of **3** having two isopropyl groups (Figure 2c), two substituted pyridine rings occupy the *trans* sites to each other with the intramolecular hydrogen bond between the coordinated amide oxygen and the N-H hydrogen of the uncoordinated amide moiety (3.041(6) Å) in a similar manner to those in **1** and **2**. This observation suggests that the formation of the intramolecular hydrogen bond provides the asymmetric coordination environments of those complexes and convergence of the naphthalene rings to form intramolecular van der Waals interactions.

A Ru(II) complex having a monoamide-TPA ligand has been also synthesized employing (1-Naph)-TPA as a ligand. The crystal structure of the cation moiety of **4** is presented in Figure 2d. The (1-Naph)-TPA ligand coordinates to the Ru(II) center as a tetradentate ligand without the coordination of its amide oxygen as observed in Ru(II)-bisamide-TPA complexes mentioned above. The amide-substituted pyridine ring occupies the *trans* position to one of the unsubstituted pyridine rings. The chloride anion binds to the Ru(II) ion at the *trans* site to the tertiary amino group; the DMSO molecule binds to Ru(II) ion with the S atom at the *trans* site to the unsubstituted pyridine ring. The intramolecular hydrogen bond can be observed between the N-H group of the amide moiety and the chloride ligand (Cl1···N5, 3.135(3) Å). Complex **4** shows a larger dihedral angle between the amide plane and the 1-naphthyl group of 57.65(4)° than those (39.3° and 45.6°) of **1**.

As an important characteristics of the Ru(II)-bisamide-TPA complexes **1 – 3**, the coordinated amide moiety can exhibit reversible deprotonation and protonation, as depicted in Scheme 1, to regulate the redox potential of the Ru^{II}/Ru^{III} couple of the ruthenium center: The redox potential can be reversibly controlled in the range of ~500 mV (500 mV for **1**, 450 mV for **2**, and 480 mV for **3**) in CH_3CN.

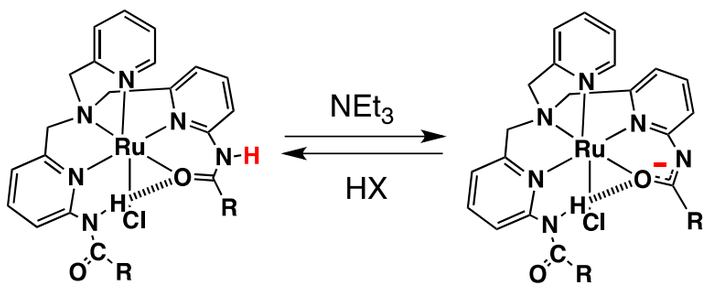

R = 1-naphthyl, 2-naphthyl, and isopropyl

Scheme 1. Reversible deprotonation and protonation of the coordinated amide moiety.

2.2 Crystal structures of ruthenium(II)-TPA-β-diketonato complexes and intramolecular rearrangement of coordination geometry of β-diketonato ligands

The convergence of functional groups to form hydrophobic environments in the coordination sphere of Ru(II) complexes has been achieved by introduction of naphthoylamide groups to the TPA ligand. Then, the ability to form π-π and CH/π (Nishio & Hirota, 1989) interactions in coordination spheres to regulate the stereochemistry of Ru centers has been examined using the Ru(II)-$(1\text{-Naph})_2$-TPA complex (**1**) and β-diketones, such as acetyl acetone (Hacac), dibenzoylmethane (Hdbm), and benzoyl acetone (Hbac). The reactions between **1** and β-diketones have been performed in ethylene glycol at 100°C in the presence of 2,6-lutidine as a base to afford corresponding β-diketonato complexes, $[Ru(acac)((1\text{-Naph})_2\text{-TPA})]PF_6$ (**5**), $[Ru(dbm)((1\text{-Naph})_2\text{-TPA})]PF_6$ (**6**), and $[Ru(bac)((1\text{-Naph})_2\text{-TPA})]PF_6$ ($\mathbf{7_{Me}}$ and $\mathbf{7_{Ph}}$) as depicted in Figure 1 (Kojima *et al.*, 2004b). In those complexes, in contrast to the case of **1**, the $(1\text{-Naph})_2$-TPA ligand coordinates to the Ru(II) center as a tetradentate ligand by the TPA moiety, and the β-diketonato ligands bind to it as bidentate monoanionic ligands. Both of the amide oxygens in the $(1\text{-Naph})_2$-TPA ligand direct to the opposite sides from the metal center and both of the amide N-H hydrogens

form intramolecular hydrogen bonds with one of the oxygen atoms of the β-diketonato ligand.

In the structure of **5** (Figure 4a), one of the methyl group of the acac ligand is sandwiched between the two naphthalene rings of the (1-Naph)$_2$-TPA ligand and forms CH/π interactions with the shortest distance of 3.34 Å for C41···C32 (Table 2 and Figure 5a). The formation of the CH/π interactions is also demonstrated in solution by ^{1}H NMR measurements in CD_2Cl_2. The singlet assigned to the included methyl protons of the acac ligand shows a large upfield shift to δ = –0.27 ppm compared to that of the nonincluded methyl group (δ = 1.86 ppm) due to the shielding by the π electrons of the naphthalene rings.

Crystal structure of **6** shows inclusion of one of the two phenyl groups of the dbm ligand in the hydrophobic cavity made of the two 1-naphthyl groups (Figure 4b). Close contact can be observed between the included phenyl ring of dbm and the naphthalene rings to form intramolecular π-π interactions (Table 2). The dihedral angles between the included phenyl ring of the dbm ligand and the two naphthalene rings are estimated to be 11.3(7)^o and 62.4(8)^o, indicating that one of the π-π interactions between them is a face-to-face type and the other isedge-to face (Figure 5b). In ^{1}H NMR measurements in CD_2Cl_2, large upfield shifts of signals assigned to the included phenyl protons compared to those of the nonincluded phenyl group are observed at δ = 5.54, 6.12, 6.50 ppm. This observation indicates the insertion of the phenyl ring into the two naphthalene rings even in solution.

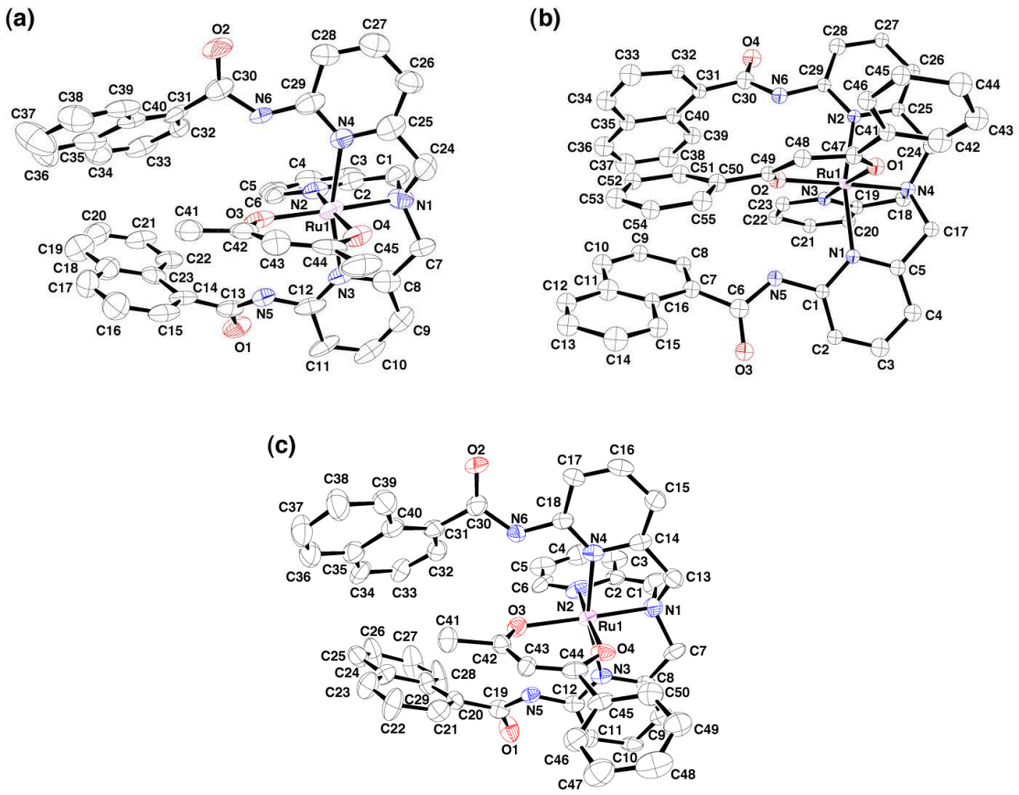

Fig. 4. ORTEP drawings of (a) **5** and (b) **6** with 50 % probability thermal ellipsoids and (c) $\mathbf{7_{Me}}$ with 30 % probability thermal ellipsoid.

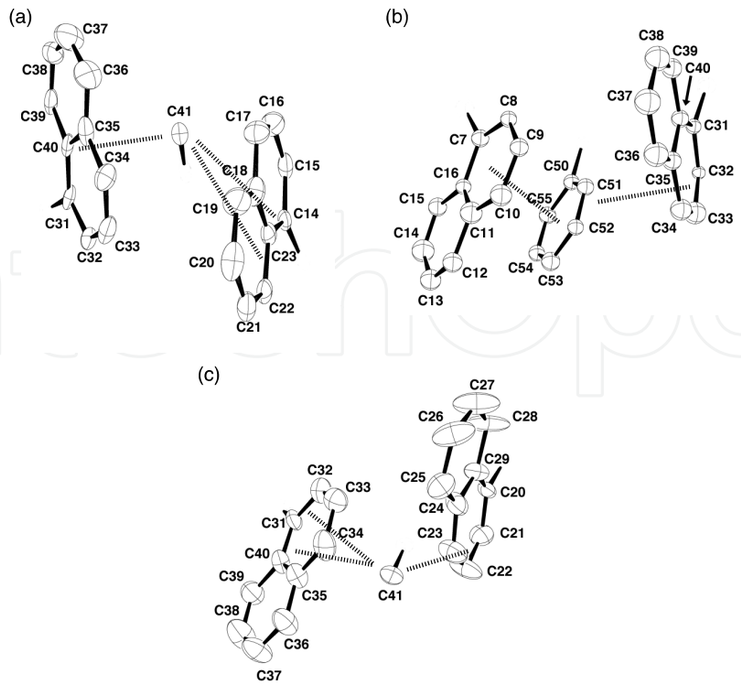

Fig. 5. Intramolecular CH/π and π-π interactions of (a) **5**, (b) **6**, and (c) $\mathbf{7_{Me}}$.

	5		6		7_{Me}
CH/π interactions		π–π interactions		CH/π interactions	
C41···C14	3.59	C51···C7	3.46	C41···C21	3.38
C41···C22	3.62	C51···C8	3.45	C41···C22	3.41
C41···C23	3.45	C51···C9	3.66	C41···C31	3.51
C41···C32	3.34	C52···C9	3.66	C41···C32	3.66
C41···C33	3.52	C52···C10	3.31	C41···C40	3.64
		C52···C16	3.42		
		C53···C11	3.35		
		C53···C12	3.43		
		C53···C13	3.62		
		C53···C15	3.69		
		C54···C14	3.59		
		C51···C32	3.36		
		C51···C33	3.48		
		C52···C33	3.47		
hydrogen bonds					
O3···N5	2.79	O2···N5	2.87	O3···N5	2.87
O3···N6	2.85	O2···N6	2.92	O3···N6	2.92

Table 2. Interatomic distances (Å) for intramolecular π–π interactions in **5**, **6**, and $\mathbf{7_{Me}}$.

The structure of $\mathbf{7_{Me}}$ has been determined as shown in Figure 4c. The methyl group of the bac ligand is also included between the two naphthyl groups as observed in the structure of

5 (Table 2 and Figure 5c). Although the single crystal of $\mathbf{7_{Ph}}$ could not be obtained, the van der Waals interaction between the substituents of bac and naphthalene rings has been indicated by large upfield shift of the methyl signal of $\mathbf{7_{Me}}$ and those of the phenyl signals of $\mathbf{7_{Ph}}$ in their ^{1}H NMR spectra.

The formation of CH/π and π-π interactions in the hydrophobic cavity made of the two naphthyl groups in the Ru(II) coordination sphere has been demonstrated for **5** with acac having two methyl groups and **6** with dbm having two phenyl groups, respectively. Then, the selectivity between π-π and CH/π interactions has been examined by using an asymmetric β-diketone, Hbac, which has both methyl and phenyl groups. After the reaction of **1** with Hbac for 3 h at 100 °C in ethylene glycol, all the starting material was consumed and a mixture of $\mathbf{7_{Me}}$ and $\mathbf{7_{Ph}}$ was obtained at the ratio of 1.8 to 1, accompanying the dissociation of the amide oxygen in **1**. This observation indicates no kinetic selectivity in the coordination mode of the bac ligand to the Ru(II) ion. However, continuous heating of this mixture of the two isomers gave only $\mathbf{7_{Me}}$ due to the selective conversion of $\mathbf{7_{Me}}$ to $\mathbf{7_{Ph}}$, indicating that $\mathbf{7_{Me}}$ is thermodynamically more favored relative to $\mathbf{7_{Ph}}$. The reaction rate of the conversion from $\mathbf{7_{Me}}$ to $\mathbf{7_{Ph}}$ has been revealed to be independent of the Hbac concentration. This result indicates that the isomerization reaction proceeds as a one-directional intramolecular rearrangement. Kinetic analysis of the rearrangement in light of Arrhenius equation has been made to determine the activation energy to be 52 kJ mol^{-1}. A proposed reaction mechanism involving a putative transition state is described in Figure 6 (Kojima *et al.*, 2004b). This intramolecular rearrangement is assumed to proceed without bond rupture and the transition state should involve weakened coordination bonds for the bac ligand.

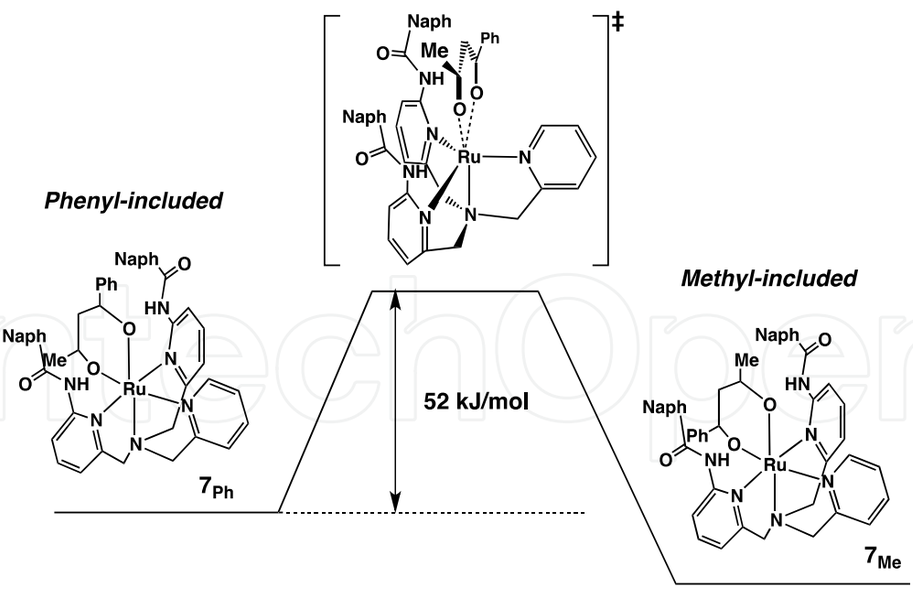

Fig. 6. A proposed reaction mechanism of the selective intramolecular rearrangement from $\mathbf{7_{Me}}$ to $\mathbf{7_{Ph}}$ in ethylene glycol.

We have also examined whether the selectivity of $\mathbf{7_{Me}}$ is derived from electronic or steric effect. According to PM3 calculation, the two oxygen atoms of bac exhibits no significant difference in its negative charges (–0.466 for Ph-C*O*- and –0.476 for Me-C*O*-), suggesting the

electronic effect is not a determining factor of the regioselectivity of $\mathbf{7_{Me}}$. The reaction of **1** with an equimolar mixture of Hacac and Hdbm has been examined to evaluate the steric effect of methyl and phenyl groups on the selective conversion to $\mathbf{7_{Me}}$. After the reaction in ethylene glycol at 100 °C for 24 h, complexes **5** and **6** were obtained in the ratio of 4.8:1. This accessibility of the methyl group in the hydrophobic cavity of the complex suggests that the steric effect may contribute to the regioselectivity. However, the complete conversion of **6** to **5** has not been observed unlike the intramolecular rearrangement from $\mathbf{7_{Ph}}$ to $\mathbf{7_{Me}}$. Therefore, the conversion from $\mathbf{7_{Ph}}$ to $\mathbf{7_{Me}}$ is supposed to be consequences of both the steric effect and the thermodynamic preference of CH/π interactions over π-π interactions in the hydrophobic cavity of the Ru(II)-(1-Naph)$_2$-TPA complex, even though superior thermodynamic stability gained by π-π interactions to that obtained by CH/π interactions is generally accepted (Steed & Atwood, 2000). The introduction of the 1-naphtyl groups attached to the TPA ligand via amide linkage has allowed us to regulate the stereochemistry of the ruthenium complex by selective inclusion of the methyl group of the bac ligand by virtue of the intramolecular CH/π interaction as well as the steric effect. The preference of CH/π interaction observed here can be attributed to the polarization of the C-H bond of the methyl group of the bac ligand bound to the positively charged Ru(II) center, making the C-H bond more acidic to strengthen the interaction between the positively polarized hydrogen atom and the negatively charged π-electron cloud of the naphthyl group.

3. Ferrocene-appended TPA derivatives and their ruthenium complexes: Intramolecular magnetic interactions between ruthenium and iron centers induced by oxidations

Ferrocene is a well-known redox-active molecule and has been introduced to many kinds of functional molecules. Among those, ferrocene-containing ligands have been reported on their multiple redox behavior and mixed-valence states toward a construction of redox-responsive functional molecules. Thus, we have prepared ferrocene-appended TPA derivatives (*N*-(6-ferrocenoylamide-2-pyridylmethyl)-*N*,*N*-bis(2-pyridylmethyl)amine = Fc-TPA, and *N*,*N*-bis(6-ferrocenoylamide-2-pyridylmethyl)-*N*-(2-pyridylmethyl)amine = Fc$_2$-TPA) and their Ru(II) complexes. We have focused on intramolecular magnetic interactions between the Fe(III) center in the ferrocenium moiety and the Ru(III) center upon oxidation. (Kojima *et al.*, 2008)

3.1 Crystal structures of a ferrocene-appended TPA derivative and its ruthenium(II) complex

In the crystal of Fc-TPA (Figure 7a), two adjacent molecules form intermolecular hydrogen bonds with each other between the amide N-H and one of unsubstituted pyridine rings (3.042(2) Å for N2···N5′, 160.5° for N2–H1′–N5′). An intermolecular C-H···O hydrogen bond is also found between the amide oxygen and one of unsubstituted pyridine ring (3.334(2) Å for C21···O1; Figure 8a). Intermolecular π-π interactions are observed between a pyridine ring and a substituted cyclopentadienyl (Cp) ring, a nonsubstituted Cp ring and adjacent pyridine rings, and a substitute pyridine ring and nonsubstituted pyridine ring (3.325(4) Å for C14···C7, 3.638(3) Å for C19···C1, 3.618(4) Å for C22···C4, 3.257(3) Å for C12-C28; Figure 8b). The π-planes of the substituted pyridine ring, the amide plane, and the amide-linked Cp

ring show a high coplanarity with the dihedral angle of 18.1° between the pyridine plane and the amide plane and 7.4° between the amide plane and the Cp ring due to the extended conjugation of π-systems.

The coordination geometry of [RuCl(Fc-TPA)(DMSO)]PF_6 **(8)** has been revealed to be similar to that of **4** (Figure 7b). The six coordination sites of the Ru(II) center of **8** are occupied by Fc-TPA as a tetradentate ligand, one chloride ion, and one DMSO molecule coordinating via the S atom. The high coplanarity of the substituted pyridine ring–the amide plane-the linked Cp ring observed in the free ligand is retained after the formation of the Ru(II) complex: The dihedral angle between the substituted pyridine ring and the amide plane is 22.8° and that between the amide plane and the Cp ring is 13.7°. An intramolecular hydrogen bond is observed between the chloride and the amide N-H hydrogen. The separation between the Ru(II) center and the Fe(II) center has been determined to be 6.656Å.

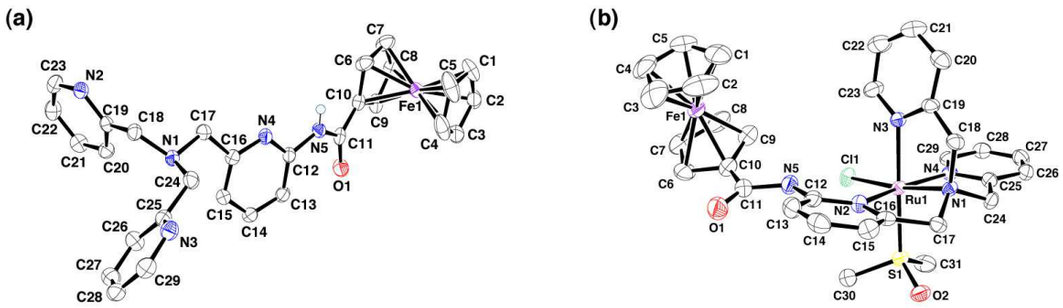

Fig. 7. ORTEP drawings of (a) Fc-TPA and (b) the cationic moiety of **8** with 50% probability thermal ellipsoids. Hydrogen atoms are omitted for clarity.

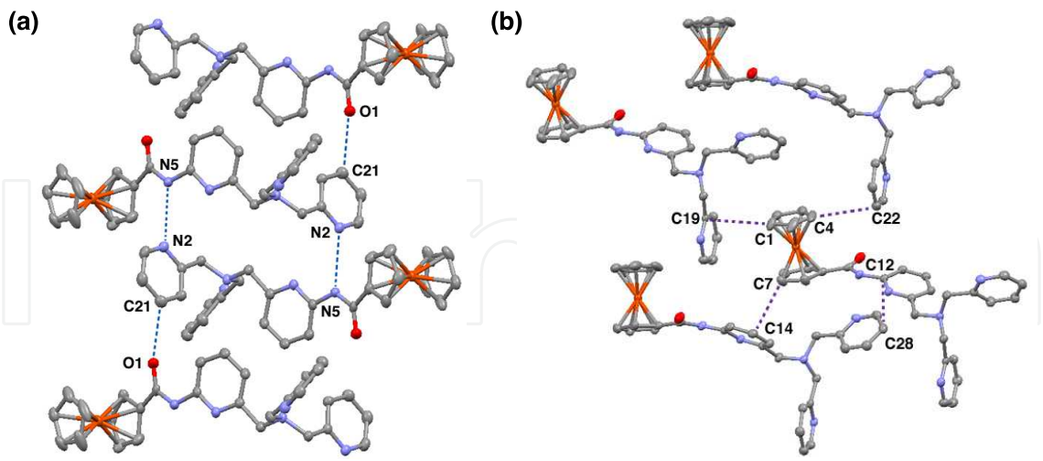

Fig. 8. Intermolecular interactions found in the crystal structure of Fc-TPA: (a) Intermolecular hydrogen bonds and (b) Intermolecular π-π interactions.

3.2 Redox behavior of ferrocene-appended ruthenium(II)-TPA complexes

In order to examine the redox properties of Fc-TPA, Fc_2-TPA, **8**, and [RuCl(Fc_2-TPA)](PF_6) **(9)** that has been proposed to possess the same geometry as those of **1–3** with one

coordinated amide oxygen, cyclic voltammetry (CV) has been performed in CH_3CN containing 0.1 M TBAP as an electrolyte at room temperature. Redox potentials were determined relative to the ferrocene/ferrocenium ion couple as 0 V.

The cyclic voltammograms of Fc-TPA and Fc_2-TPA showed reversible redox waves at $E_{1/2}$ = 0.21 V and 0.23 V assigned to the Fc/Fc^+ couples, respectively.

The CV of **8** showed two redox waves at 0.23 V (ΔE = 86 mV) and 0.77 V (ΔE = 159 mV) at 100 mv/s. The first redox wave has been assigned to the Fc/Fc^+ couple of the coordinated Fc-TPA based on the redox potential of the free Fc-TPA. The redox potential of the second one is similar to that of **4** (0.79 V for Ru^{II}/Ru^{III}), therefore the second redox process has been assigned to the Ru^{II}/Ru^{III} couple. The Ru^{II}/Ru^{III} couple has exhibited a change of peak current with altering the scan rate, suggesting that this process is quasi-reversible.

Complex **9** shows reversible redox waves at 0.27 V and 0.46 V at the scan rate of 20 mV/s. The peak current of the first wave is twice as large as the second one. Thus, the first peak can be assigned to an overlapped wave derived from the Fc/Fc^+ couple of the uncoordinated Fc-amide moiety and the Ru^{II}/Ru^{III} couple based on the redox potential of Fc_2-TPA and **3** (0.27 V for Ru^{II}/Ru^{III}) and Ru(II)-bisamide-TPA (0.34 V for **1**, 0.30 V for **2**, and 0.27 V for **3**). The second redox couple was assigned to the Fc/Fc^+ couple of the coordinated Fc-amide moiety. The redox potentials of the two Fc moieties have been separated due to the coordination of the amide oxygen of one of the Fc-amide arms in **9**.

3.3 Magnetic interaction between the Ru(III) center and the Fe(III) center in ferrocene-appended ruthenium(II)-TPA complexes

We examined intramolecular magnetic interactions between the Ru center and the Fe center in **8** and **9** upon oxidation by $[Ru(bpy)_3]^{3+}$ in CH_3CN. Variable-temperature EPR spectra of two-electron oxidized species of **8**, $[Ru^{III}Cl(Fc^+\text{-TPA})^+(DMSO)]^{3+}$, showed a signal derived from a forbidden transition (Δm_s = 2) in a triplet state at g = 4.28 and a signal due to an allowed transition (Δm_s = 1) at g = 2.0038. The obtained EPR spectrum is different from reported EPR signal of Fc^+ with $g_{//}$ = 4.36 and $g_{\perp}$ = 1.30 in acetone at 20 K (Prins & Reinders, 1969) and also the EPR signal of the one-electron oxidized species of Fc-TPA with an intense signal at g = 2.0186 and a weak signal at g = 4.22 in CH_3CN at 2.6 K. The intensity of the signal at g = 4.28 of $[Ru^{III}Cl(Fc^+\text{-TPA})^+(DMSO)]^{3+}$ increased as lowering temperature as shown in Figure 9a. Therefore, the ground state of the two-electron oxidized species should be a triplet state (S = 1). A ferromagnetic coupling constant has been estimated to be J = 13.7 cm^{-1} based on the Bleaney-Bowers equation (Bleaney & Bowers, 1952) using the temperature-dependent change of the intensity of the signal at g = 4.28 (see Figure 9b) (Kojima *et al.*, 2008).

In order to gain structural insights into the triplet state, we have applied DFT calculations to optimize the structure of the two-electron oxidized species of **8** in the S = 1 state. The optimized structure has longer interatomic distance between Ru(III) center and Fe(III) center (7.523 Å) than that observed in the crystal structure of **8** (6.656 Å). The dihedral angle between the amide plane and the Cp ring (42.8°) has enlarged compared to that in the crystal structure of **8**. The calculated spin densities at the Ru(III) center (+0.925) and Fe(III) center (+1.397) suggests the localization of unpaired electrons at those metal centers. We assumed that the ferromagnetic interaction between Ru(III) and Fe(III) centers was induced by a superexchage interaction through the amide linkage (Kojima *et al.*, 2008).

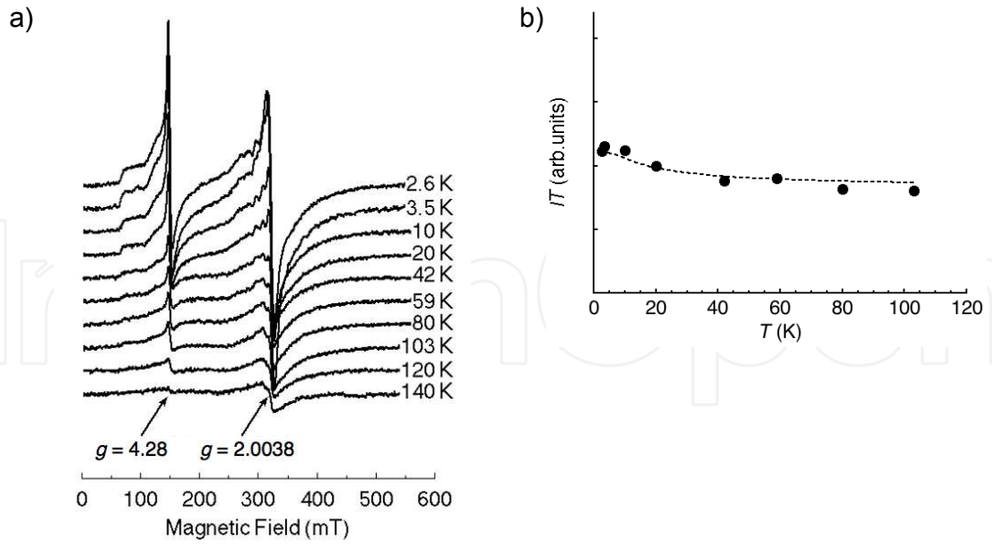

Fig. 9. (a) Variable-temperature EPR spectra of the two-electron oxidized species of **8** in the range of 2.6 – 140 K in CH_3CN. (b) Temperature dependence of *IT* (*I* reporesents the integration intensity of the signal at g = 4.28) of the two-electron oxidized species of **8**, together with the curve-fit of the data to the Bleaney-Bowers equation.

EPR measurements of **9** have been also made in CH_3CN at –150°C. In the case of its two-electron oxidation, the uncoordinated Fc and the Ru center of **9** can be oxidized according to the CV measurement, and the product ($[Ru^{III}Cl(Fc_2\text{-TPA})^+]^{3+}$) exhibited EPR signals at g = 2.01 (Δm_s = 1) and g = 4.11 (Δm_s = 2) as observed in $[Ru^{III}Cl(Fc\text{-TPA})^+]^{3+}$, indicating the formation of a resemble triplet state to that of $[Ru^{III}Cl(Fc\text{-TPA})^+]^{3+}$.

4. Ruthenium(II)-TPA complex having catechol pendants via amide linkages

Catechol and its derivatives have been known to form stable complexes with metal ions. Introduction of catechols to TPA enables us to create a ruthenium-TPA complex having a metal binding site formed by convergence of the catechol moiety. Such compound may allow us to readily create multinuclear metal complexes with multistep redox systems involving electronic interactions among those redox centers. Thus, we have synthesized a catechol-containing TPA (*N*,*N*-bis[6-{3,4-(dihydroxy)benzamide}-2-pyridylmethyl]-*N*-(2-pyridyl-methyl)amine = $(H_2Cat)_2$-TPA) and its ruthenium complex, $[RuCl((H_2Cat)_2\text{-TPA})]Cl$ (**10**) (Kojima *et al.*, 2010).

4.1 Crystal structure of a ruthenium(II) complex with two catechol pendants via amide linkages

The coordination environment of the Ru(II) center in the structure of **10** is similar to those of other related Ru(II)-bisamide-TPA complexes in terms of the coordination of Cat_2-TPA as a pentadendate ligand involving the coordination of one amide oxygen, as depicted in Figure 10. The chloride ion binds to the Ru(II) center at the *trans* position of the unsubstituted pyridine ring as can be seen in other related complexes (see Figure 2). The coordinated amide oxygen is located at the *trans* site to the tertiary amine, and the pyridine ring linked to the coordinated amide moiety is located at the *trans* position to the other amide

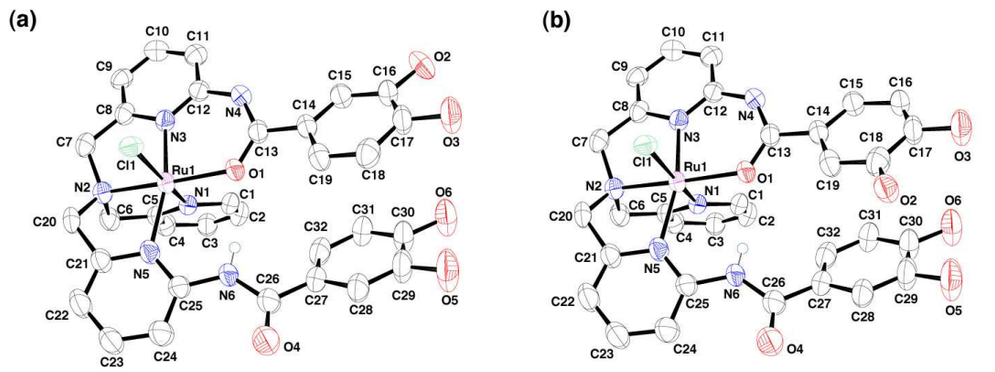

Fig. 10. ORTEP drawings of the cation moieties of two isomers A (a) and B (b) of **10**.

substituted pyridine ring to form intramolecular hydrogen bond (2.938 (7) Å for O1···N6, 148.9(4)° for O1···H-N6). Disorder of the O2 atom can be found in the catechol moiety connected to the coordinated amide arm, giving rise to two conformational (rotational) isomers in the crystal structure (Form A and B in Figure 10). The intramolecular π-π interactions between the two catechol moieties are observed in both isomers with the shortest distance of 3.36 Å. The O3 atom in the catechol rings forms a hydrogen bond with a water molecule of crystallization (2.90 Å for O3···O8). One of the oxygen atoms of the catechol moiety (O2) in the form A binds with O3 of an adjacent molecule through an intermolecular hydrogen bond with the distance of 2.637 Å (Figure 11).

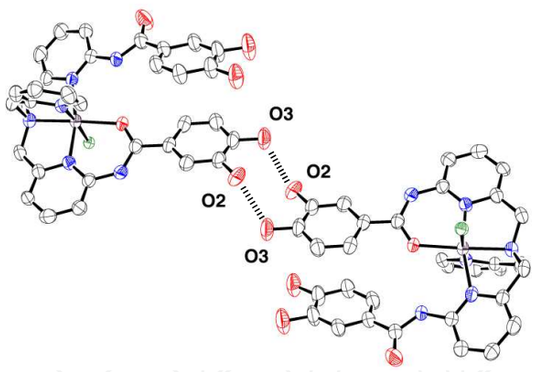

Fig. 11. Intermolecular hydrogen bonds between catechol moieties of form A of **10**.

4.2 Cu(II) binding to the converged catechol moieties to form a unique bimetallic complex

As observed in the crystal structure of **10**, the two independent catechol moieties have been successfully converged into one direction as a metal-binding site. Prior to the examination of metal binding to the catechol moieties, we have shed some lights on the deprotonation processes of **10**. The UV-vis titration of **10** with tetramethylammonium hydroxide (TMAOH) in DMF shows three-step spectral change. We assigned the first-step spectral change observed in the course of the addition of 0-2 equiv of TMAOH to the deprotonation of the coordinated amide N-H as observed for other Ru(II)-bisamide-TPA complexes (see Scheme 1 in Section 2.1) and one of the catechol O-H having lowest pK_a value as a consequence of convergence of catechol moieties (Scheme 2). The second and third deprotonation steps observed in the course

of the addition of 2-3 and 3-5 equiv of TMAOH have been assigned to deprotonation of one catechol O-H and remaining two catechol O-H protons, respectively, as shown in Scheme 2.

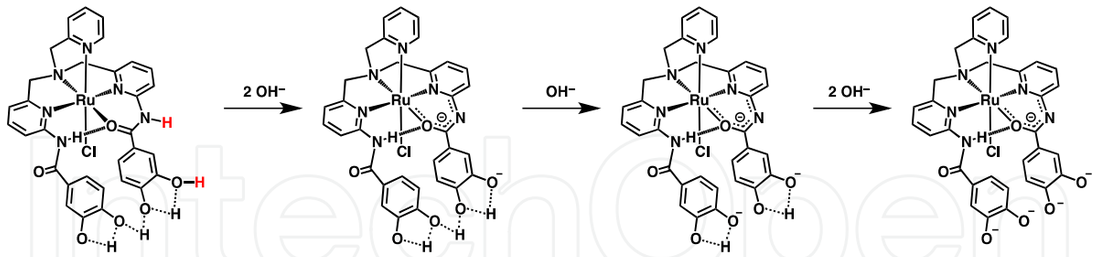

Scheme 2. Deprotonation processes of **10**.

As a precursor for the complexation of the Cu(II) ion to **10**, we have employed $[Cu^{II}(NO_3)_2(TMEDA)]$ (TMEDA = *N*,*N*,*N*′,*N*′-tetramethylethylenediamine) (Pavkovic *et al*. 1977), since the Cu(II) ion can form the most stable complex in light of the Irwing-Williams series. The UV-vis titration of **10** with $[Cu^{II}(NO_3)_2(TMEDA)]$ in MeOH allows us to reveal that the catechol moieties of **10** is capable of binding to only one Cu(II)-TMEDA unit. The reaction between **10** and $[Cu^{II}(NO_3)_2(TMEDA)]$ in MeOH proceeds in the presence of NEt_3. The addition of $TBAPF_6$ to a mixture of **10** and $[Cu^{II}(NO_3)_2(TMEDA)]$ gives a powder of $[RuCl((HCat)_2\text{-}TPA)\{Cu(TMEDA)\}]PF_6$ (**11**). ESI-MS measurements on **11** afforded a peak cluster at m/Z = 906.1 assigned to $[RuCl((HCat)_2\text{-}TPA)\{Cu(TMEDA)\}]^+$, indicating that each catechol moiety releases one proton and the converged two catechol moieties can accept one Cu(II)-TMEDA unit as demonstrated by the spectroscopic titration.

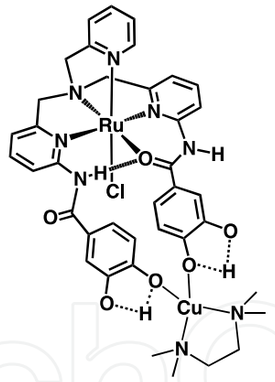

Fig. 12. Putative structure of **11**.

The EPR spectrum of **11** in MeOH at 77 K shows an anisotropic signal at $g_{//}$ = 2.239 and $g_{\perp}$ = 2.060, together with hyperfine coupling constant (hfc) of $A_{//}$ = 184 G due to Cu(II). These parameters are different from those of [Cu(catecholato)(TMEDA)] ($g_{//}$ = 2.241, $g_{\perp}$ = 2.071, and $A_{//}$ = 184 G) (Kodera *et al*., 2003), even though the signals indicate that both Cu(II) complexes are with a monomeric tetragonal geometry in the $(d_{x^2\text{-}y^2})^1$ ground state (Wojciechowski *et al*., 2009; Nielsen *et al*., 2008). Considering the deprotonation behavior of catechol moieties, the complex **11** is supposed to have a unique coordination environment of a Cu(II)-catecholate complex as described in Figure 12. DFT calculations at the B3LYP/LANL2DZ level of theory suggest that the optimized structure of **11** shown in Figure 12 is more stable in 3.5 kcal/mol than that of a bimetallic complex holding the Cu-TMEDA unit at one catecholate moiety in a bidentate fashion.

5. Summary

In this chapter, we have presented an overview of ruthenium complexes having TPA derivatives with functional groups via amide linkages. The strategy has allowed us to construct unique second coordination spheres of ruthenium complexes gaining novel functionality. The ruthenium coordination to bisamide-TPA derivatives affords the convergence of functional groups attached by the amide linkage into one direction to form specific environments, such as a hydrophobic cavity. The hydrophobic cavity made of the two naphthyl groups forms noncovalent van der Waals interactions with inserted substituents. Under this situation, we can observe the uni-directional intramolecular rearrangement based on the theromodynamic preference of CH/π interactions to π-π interactions. The introduction of ferrocene moiety to the TPA ligand makes possible intramolecular ferromagnetic interaction between Ru(III) and Fe(III) centers in the ruthenium complex with ferrocene units as pendants. A catechol-appended TPA ligand can provide a preorganized metal binding site consisting of the two catechol moieties on the ruthenium complex to accept one Cu(II) complex in a unique coordination mode. Recently, we have also prepared a TPA derivative having two 1,10-phenanthroline (phen) moieties via amide linkages and its Ru(II) complex: The complex can form two appended Ru(II)-phen complexes and perform cooperative transfer hydrogenation of ketones (Kojima *et al*., 2011). In those complexes, the intramolecular hydrogen bond formed between the amide moieties can facilitate convergence of the functional groups and stabilize the complexes. This can be a significant advantage for the development of transition-metal-based functional molecules. Thus, the design of Ru-TPA complexes having functional groups via amide linkage will provide a nice opportunity to create cooperative molecular functionality on the basis of characteristics of both the ruthenium center and functional groups to provide a unique second coordination sphere as well as other metal ions attached to the functional groups.

6. References

Bleaney, B., Bowers, K. D. (1952). Anomalous Paramagnetism of Copper Acetate. *Proc. R. Soc. London, Ser. A,* Vol.214, No.1119, pp. 451-465.

Harata, M., Jitsukawa, K., Masuda, H., Einaga, H. (1994). A Structurally Characterized Mononuclear Copper(II)-Superoxo Complex. *J. Am. Chem. Soc.*, Vol.116, No.23, pp. 10817-10818.

Harata, M., Jitsukawa, K., Masuda, H., Einaga, H. (1995). Synthesis and Structure of a New Tripodal Polypyridine Copper(II) Complex That Enables to Recognize a Small Molecule. *Chem. Lett.*, Vol.24, No.1, pp.61-62.

Harata, M., Hasegawa, K.; Jitsukawa, K., Masuda, H., Einaga, H. (1998). Preparations, Structures, and Properties of Copper(II) Complexes with New Tripodal Tetradentate Ligand. *N*-(2-Pyridylmethyl)bis(6-pyvalamido-2-pyridylmethyl)amine, and Reactivities of the Cu(I) Complex with Dioxygen. *Bull. Chem. Soc. Jpn.*, Vol. 71, No.5, pp. 1031-1038.

Hunter, C. A., Sanders, J. K. M. (1990). The Nature of π-π Interactions. *J. Am. Chem. Soc.*, Vol.112, No.14, pp. 5525-5534.

Janiak, C. (2000). A Critical Account on π-π Stacking in Metal Complexes with Aromatic Nitrogen-containing Ligands. *Inorg. Chem.*, Vol.49 No.8, pp. 3737-3745.

Kodera, M., Kawata, T., Kano, K., Tachi, Y., Itoh, S., Kojo, S. (2003). Mechanism for Aerobic Oxidation of 3,5-Di-*tert*-butylcatechol to 3,5-Di-*tert*-butyl-*o*-benzoquinone Catalyzed

by Di-μ-hydroxo-dicopper(II) Complexes of Peralkylated Ethylelnediamine Ligands. *Bull. Chem. Soc. Jpn.,* Vol.76, No.10, pp. 1957-1964.

Kojima, T., Hayashi, K., Matsuda, Y. (2000). A Ruthenium(II)-Pyridylamine Complex Showing a Fluxional Intramolecular π-π Interaction. *Chem. Lett.*, Vol.29, No.9, 1008-1009.

Kojima, T., Hayashi, K., Matsuda, Y. (2004a). Structures and Properties of Ruthenium(II) Complexes of Pyridylamine Ligands with Oxygen-Bound Amide Moieties: Regulation of Structures and Proton-Coupled Electron Transfer. *Inorg. Chem.,* Vol.43, No.21, pp. 6793-6804.

Kojima, T., Miyazaki, S., Hayashi, K., Shimazaki, Y., Tani, F., Naruta, Y., Matsuda, Y. (2004b). Intramolecular Rearrangement for Regioselective Complexation by Intramolecular CH/π Interaction in a Hydrophobic Cavity of a Ruthenium Coordination Sphere. *Chem.–Eur. J.,* Vol.10, No.24, pp. 6402-6410.

Kojima, T., Matsuda, Y. (2005). A Novel Ru(II)–DMSO Complex Having Non-coordinating 1-Naphthoylamide Arm: Effects of Intramolecular Hydrogen Bonding on Redox Potential of the Ruthenium Center. *Chem. Lett.,* Vol.34, No.2, pp. 258-259.

Kojima, T., Noguchi, D., Nakayama, T., Inagaki, Y., Shiota, Y., Yoshizawa, K., Ohkubo, K., Fukuzumi, S. (2008). Synthesis and Characterization of Novel Ferrocene-Containing Pyridylamine Ligands and Their Ruthenium(II) Complexes: Electronic Communication through Hydrogen-Bonded Amide Linkage. *Inorg. Chem.,* Vol.47, No.3, pp. 886-895.

Kojima, T., Hirasa, N., Noguchi, D., Ishizuka, T., Miyazaki, S., Shiota, Y., Yoshizawa, K., Fukuzumi, S. (2010). Synthesis and Characterization of Ruthenium(II)-Pyridylamine Complexes with Catechol Pendants as Metal Binding Sites. *Inorg. Chem.,* Vol.49, No.8, pp. 3737-3745.

Nielsen, P., Toftlund, H., Boas, J. F., Pilbrow, J. R., Moubaraki, B., Murray, K. S., Neville, S. M. (2008). Electron Paramagnetic Resonance and Crystallographic Resolution of an Axially Compressed Octahedral Complex $[Cu(terpyR8)_2](ClO_4)_2$ Containing the C_8 Alkyl-chain Ligand TerpyR8; 4′-octoxy-2,2′:6′,2′′-terpyridine. *Inorg. Chim. Acta,* Vol.361, No.12-13, pp. 3453-3461.

Nishio, M., Hirota, M. (1989). CH/π Interaction: Implications in Organic Chemistry. *Tetrahedron,* Vol.45, No.23, pp. 7201-7245.

Pavkovic, S. F., Miller, D., Brown, J. N. (1977). Dinitrato(*N*,*N*,*N*',*N*'-tetramethylethylene-diamine)copper(II). *Acta Crystallogr.,* Vol.B33, No.9, pp. 2894-2896.

Prins, R., Reinders, F. J., (1969). Electron Spin Resonance of the Cation of Ferrocene. *J. Am. Chem. Soc.,* Vol.91, No.17, pp. 4929-4931.

Steed, J., Atwood, J. (2000). *Supramolecular Chemistry,* Wiley, ISBN 978-0-470-51234-0, Chichester, UK.

Wada, A., Harata, M., Hasegawa, K., Jitsukawa, K., Masuda, H., Mukai, M., Kitagawa, T., Einaga, H. (1998) Structural and Spectroscopic Characterization of a Mononuclear Hydroperoxo-Copper(II) Complex with Tripodal Pyridylamine Ligands. *Angew. Chem., Int. Ed.*, Vol.37, No.6, 798-799.

Wojciechowski, K., Bitner, A., Bernardinelli, G., Brynda, M. (2009). Azacrown Ether–Copper(II)–hexanoate Complexes. From Monomer to 1-D metal Organic Polymer. *Dalton Trans.*, No.7, pp. 1114-1122.

Yano, Y., Kojima, T., Fukuzumi, S. (2011). Cooperative Catalysis of a Trinuclear Ruthenium(II) Complex in Transfer Hydrogenation of Ketones by Formic Acid. *Inorg. Chim. Acta*, Vol. 374, No. 1, pp. 104-111.

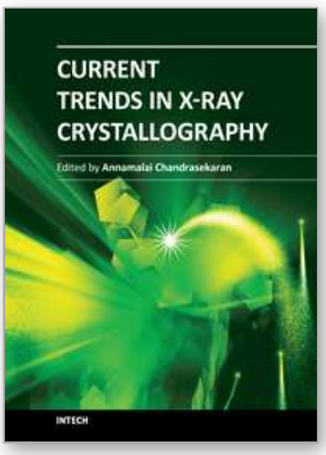

Current Trends in X-Ray Crystallography

Edited by Dr. Annamalai Chandrasekaran

ISBN 978-953-307-754-3

Hard cover, 436 pages

Publisher InTech

Published online 16, December, 2011

Published in print edition December, 2011

This book on X-ray Crystallography is a compilation of current trends in the use of X-ray crystallography and related structural determination methods in various fields. The methods covered here include single crystal small-molecule X-ray crystallography, macromolecular (protein) single crystal X-ray crystallography, and scattering and spectroscopic complimentary methods. The fields range from simple organic compounds, metal complexes to proteins, and also cover the meta-analyses of the database for weak interactions.

How to reference

In order to correctly reference this scholarly work, feel free to copy and paste the following:

Soushi Miyazaki and Takahiko Kojima (2011). Ruthenium(II)-Pyridylamine Complexes Having Functional Groups via Amide Linkages, Current Trends in X-Ray Crystallography, Dr. Annamalai Chandrasekaran (Ed.), ISBN: 978-953-307-754-3, InTech, Available from: http://www.intechopen.com/books/current-trends-in-x-ray-crystallography/ruthenium-ii-pyridylamine-complexes-having-functional-groups-via-amide-linkages

INTECH
open science | open minds

InTech Europe
University Campus STeP Ri
Slavka Krautzeka 83/A
51000 Rijeka, Croatia
Phone: +385 (51) 770 447
Fax: +385 (51) 686 166
www.intechopen.com

InTech China
Unit 405, Office Block, Hotel Equatorial Shanghai
No.65, Yan An Road (West), Shanghai, 200040, China
中国上海市延安西路65号上海国际贵都大饭店办公楼405单元
Phone: +86-21-62489820
Fax: +86-21-62489821

IntechOpen